Journal of Molecular Spectroscopy **208,** 136–143 (2001)
doi:10.1006/jmsp.2001.8371, available online at http://www.idealibrary.com on IDEAL®

The Near Ultraviolet Band System of Singlet Methylene

S. N. Yurchenko,* Per Jensen,* Yan Li,* R. J. Buenker,* and P. R. Bunker†

*Fachbereich 9, Theoretische Chemie, Bergische Universität–Gesamthochschule Wuppertal, D-42097 Wuppertal, Germany; and †Steacie Institute for Molecular Sciences, National Research Council of Canada, Ottawa, Ontario K1A 0R6, Canada

Received April 2, 2001

In a classic paper by G. Herzberg and J. W. C. Johns entitled "The Spectrum and Structure of Singlet CH_2" (*Proc. Roy. Soc. A* **295**, 107–128 (1966)) the analysis of the $\tilde{b}\,^1B_1 \leftarrow \tilde{a}\,^1A_1$ red absorption band system of CH_2 is discussed in detail for the first time. In addition to that band system the observation of a fragment of a weak near ultraviolet absorption band system is reported. The three observed bands of the system could not be vibrationally assigned or rotationally analyzed but it was pointed out that they probably involve absorption into the second excited singlet state, $\tilde{c}\,^1A_1$. We show this supposition to be true here by simulation. In order to simulate the spectrum we have calculated *ab initio* the $\tilde{c}$–$\tilde{a}$ and $\tilde{c}$–$\tilde{b}$ transition moment surfaces and used the MORBID and RENNER program systems with previously determined potential energy surfaces for the $\tilde{a}$, $\tilde{b}$, and $\tilde{c}$ states in a calculation of the energy levels and wavefunctions. We find that the three bands seen by Herzberg and Johns are part of the $\tilde{c} \leftarrow (\tilde{a}/\tilde{b})$ system but that all of the bands of the system above about 31 000 cm^{-1} are missing as a result of $\tilde{c}$ state predissociation. We vibrationally assign the bands but the weakness of the spectrum, and the presence of perturbations, make it impossible for us to analyze the rotational structure fully. Further experimental and theoretical studies are suggested. © 2001 Academic Press

Key Words: CH_2; near ultraviolet; band system.

I. INTRODUCTION

In 1966 Herzberg and Johns (*1*) published the analysis of the $\tilde{b}\,^1B_1 \leftarrow \tilde{a}\,^1A_1$ absorption band system of methylene (CH_2) that had been obtained by flash photolysis of diazomethane (CH_2N_2). Since that time the $\tilde{b}$–$\tilde{a}$ band system of CH_2 has been much studied both experimentally and theoretically (see (*2*) and references therein) because of the importance of the methylene radical as a chemical intermediate. Theoretical interest arises because the $\tilde{a}$ and $\tilde{b}$ states of CH_2 correlate with a $^1\Delta_g$ state at linearity and are therefore involved in a Renner–Teller interaction; the most recent theoretical study of this system is in (*3*). In (*1*) Herzberg and Johns also reported the observation of a fragment of a near ultraviolet electronic band system which they were unable to analyze. They said that the upper state of the system was probably the predicted excited $^1A_1$ electronic state that corresponds to a $^1\Sigma_g^+$ state at linearity, i.e., the $\tilde{c}\,^1A_1$ electronic excited state. In the present paper we show that this supposition is true, but that predissociation in the $\tilde{c}$ state must be invoked to account for the fact that bands above about 31 000 cm^{-1} are missing.

In (*1*) the lines of the near ultraviolet system are said to be rather weak, and the appearance of the strongest region of the system given in Fig. 2 of (*1*) supports that assertion. In Table 3 of (*1*) the vacuum wavenumbers of the lines are given together with their intensities as simply estimated from the darkness of the lines on the photographic plates; the intensities are represented by the values 0 (for barely observable lines) through 4 (for the darkest lines).[1] Using this information we have drawn a stick spectrum of the band system and it is given here in Fig. 1. The aim of the present paper is to reconcile our simulation of the $\tilde{c}\,^1A_1 \leftarrow (\tilde{a}\,^1A_1/\tilde{b}\,^1B_1)$ band system with this observed spectrum. In order to simulate the spectrum we have calculated *ab initio* the $\tilde{c}$–$\tilde{a}$ and $\tilde{c}$–$\tilde{b}$ transition moment surfaces, and used the MORBID (*4–7*) and RENNER (*8–10*) program systems with previously determined potential energy surfaces for the $\tilde{a}$ (*3*), $\tilde{b}$ (*3*), and $\tilde{c}$ (*11*) states in a calculation of the energy levels and wavefunctions.

Cross-sections through the potential surfaces of the $\tilde{a}$, $\tilde{b}$, and $\tilde{c}$ states showing their dependence on the bond angle supplement ρ are given in Fig. 2; the $\tilde{a}$ and $\tilde{b}$ state potentials are from Table 3 of (*3*) and the $\tilde{c}$ state potential is from Table 2 of (*11*). The bond lengths are held fixed at their respective equilibrium values for each state. In the figure we show the two lowest singlet state dissociation limits, $[CH(X^2\Pi; v = N = 0) + H(^2S)]$ and $[C(^1D) + H_2(X^1\Sigma_g^+; v = J = 0)]$, as well as the energy region of the $\tilde{c}$ state levels observed in (*1*). The position of the $[(0, 0, 0), J = 0]$ level of the $\tilde{a}\,^1A_1$ state is also indicated. The energy zero in Fig. 2 is that of the $[(0, 0, 0), N = 0]$ level of the $\tilde{X}\,^3B_1$ state so that the energy of the $[(0, 0, 0), J = 0]$ level of the $\tilde{a}$-state is the singlet–triplet splitting, $T_0(\tilde{a}) = 3147$ cm^{-1} (*12*).

[1] In a private communication Dr. Johns has informed us that these intensity numbers are based on the darkness of the lines on each of the photographic plates, and that such darkness is not a linear function of the spectroscopic intensity of a line; they do indicate the order of the intensities of the lines within each band.

0022-2852/01 $35.00
Copyright © 2001 by Academic Press
All rights of reproduction in any form reserved.

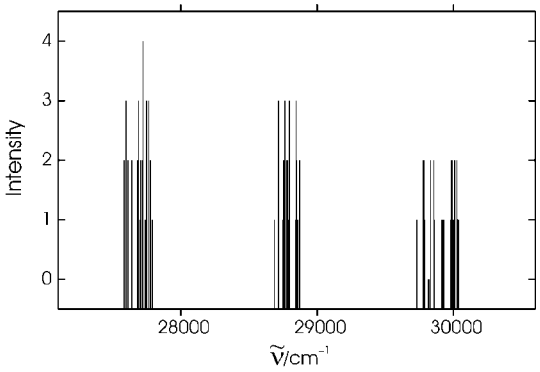

FIG. 1. A stick spectrum of the near ultraviolet band system obtained in (*1*), which we have drawn based on the vacuum wavenumbers and intensities given in Table 3 of (*1*).

II. THE TRANSITION MOMENT SURFACES

The *ab initio* calculation of the $\tilde{c} \leftarrow \tilde{a}/\tilde{b}$ transition moments has been carried out using the multireference single- and double-excitation configuration–interaction method (MRD-CI (*13*, *14*)) employing a direct-CI approach (*15*) based on the Table-CI algorithm (*16–18*). The atomic orbital basis set used is the same as described in (*3*) and is of cc-pVQZ quality (*19*). The first step in the calculations is to carry out a restricted Hartree–Fock treatment of the $\tilde{X}\ ^3B_1$ ground state. The resulting molecular orbitals are then employed as the orthonormal one-electron basis for all subsequent CI calculations. A total of 50 nuclear geometries have been considered, covering bond angles between 80° and 180° and C–H bond distances ranging from 0.864 to 1.364 a_0; C_s symmetry is assumed throughout, with the $\tilde{a}$ and $\tilde{c}$ states belonging to the A' irreducible representation, and $\tilde{b}$ to A''.

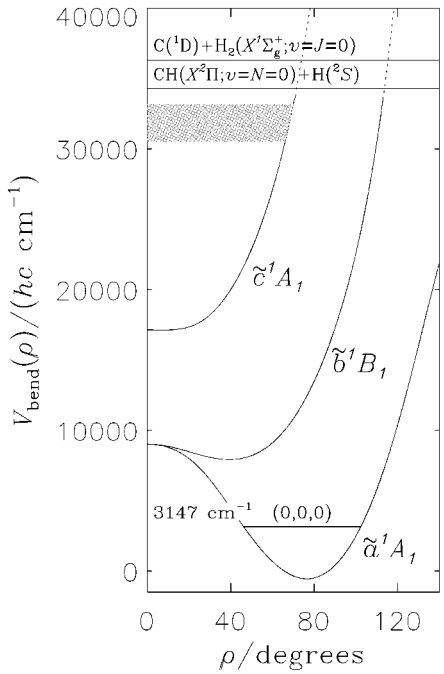

FIG. 2. The bending potentials for the $\tilde{a}$ and $\tilde{b}$ states (from (*3*)) and for the $\tilde{c}$ state (from (*11*)). The two lowest singlet state dissociation limits and the energy of the lowest level in the $\tilde{a}$ state are also given; the energy zero is that of the energy of the lowest level of the $\tilde{X}\ ^3B_1$ state. The shaded area shows the energy region in which the $\tilde{c}$ state levels were observed in (*1*).

The CI calculations employ a configuration selection scheme (*13*, *15*) with a threshold of 0.8 nanohartree. The resulting configuration spaces are typically of order 88 125 ($^1A'$) and 165 700 ($^1A''$) spin-adapted functions and the two lowest roots each of A' and A'' symmetry have been extracted from the corresponding secular equations. The corresponding reference configurations were chosen in a self-consistent manner based on the coefficients for the CI wavefunctions (34 for $^1A'$ and 66 for $^1A''$). Transition moments for all three components of the electric dipole operator, $\sum_i e_i \mathbf{r}_i$, have been computed by employing the corresponding variational wavefunctions. In addition, dipole moments have been computed for each of the above four states at all the above nuclear geometries. The corresponding potential energy data were also compared with those reported in Ref. (*11*) and found to be in good agreement, thereby establishing that the present transition and dipole results have been obtained at a level consistent with the quality of the *ab initio* potential energy surfaces employed.

We describe the transition dipole moment in terms of its components along three axes xqp (taken to form a right-handed axis system with origin in the nuclear center of mass) which are attached directly to the instantaneous nuclear configuration of the molecule (see Fig. 1 of Ref. (*6*)). For CH_2, the q axis bisects the bond angle $\angle$ (HCH) and is directed so that the q coordinates of the H nuclei 1 and 3 are positive. The p axis is perpendicular to the q axis and its direction is such that the p coordinate of nucleus 3 is positive, and the x axis is perpendicular to the molecular plane.

The electronic integrals $\langle\psi_{\rm elec}^{(\tilde{c})}|\mu_\alpha|\psi_{\rm elec}^{(\sigma)}\rangle_{\rm el}$, where $\alpha = x, q, p$, while $\sigma = \tilde{a}$ or $\tilde{b}$ and the subscript 'el' signifies that integration is over the electronic coordinates only, depend solely on the vibrational coordinates $(\Delta r_{12}^{(\rm ref)}, \Delta r_{32}^{(\rm ref)}, \bar{\rho})$, where $\Delta r_{j2}^{(\rm ref)} = r_{j2} - r_{j2}^{(\rm ref)}$ is the instantaneous value of the displacement of the distance r_{j2} between H nucleus $j = 1$ or 3 and the C nucleus (labeled 2) from its reference value $r_{j2}^{(\rm ref)}$ (see Section III for a discussion of the choice of $r_{j2}^{(\rm ref)}$), and $\bar{\rho} = \pi - \angle$ (HCH). All of these vibrational coordinates have positive parity (i.e., they are unchanged by the spatial inversion operator E^* (*20*)). Consequently, in order for an electronic integral $\langle\psi_{\rm elec}^{(\tilde{c})}|\mu_\alpha|\psi_{\rm elec}^{(\sigma)}\rangle_{\rm el}$ to be nonvanishing, the integrand must have positive parity, and the nonvanishing transition dipole moments are thus

$$\bar{\mu}_p^{(\tilde{c}\tilde{a})}\left(\Delta r_{12}^{(\rm ref)}, \Delta r_{32}^{(\rm ref)}, \bar{\rho}\right) = \left\langle\psi_{\rm elec}^{(\tilde{c})}|\mu_p|\psi_{\rm elec}^{(\tilde{a})}\right\rangle_{\rm el}, \qquad [1]$$

$$\bar{\mu}_q^{(\tilde{c}\tilde{a})}\left(\Delta r_{12}^{(\rm ref)}, \Delta r_{32}^{(\rm ref)}, \bar{\rho}\right) = \left\langle\psi_{\rm elec}^{(\tilde{c})}|\mu_q|\psi_{\rm elec}^{(\tilde{a})}\right\rangle_{\rm el}, \qquad [2]$$

and

$$\bar{\mu}_x^{(\tilde{c}\tilde{b})}\left(\Delta r_{12}^{(\rm ref)}, \Delta r_{32}^{(\rm ref)}, \bar{\rho}\right) = \left\langle\psi_{\rm elec}^{(\tilde{c})}|\mu_x|\psi_{\rm elec}^{(\tilde{b})}\right\rangle_{\rm el}. \qquad [3]$$

Copyright © 2001 by Academic Press

In the *ab initio* calculations, the values of these three electronic integrals are calculated at each nuclear geometry. However, since the calculations at each geometry are independent of each other, the phases of the electronic wavefunctions $\psi_{\text{elec}}^{(\tilde{a})}$, $\psi_{\text{elec}}^{(\tilde{b})}$, and $\psi_{\text{elec}}^{(\tilde{c})}$ can vary between geometries in an arbitrary way. In practice, these wavefunctions are real, and so only their signs can vary. Such sign variations lead to arbitrary sign changes in the electronic integrals as the nuclear geometry changes. We must obtain values of these integrals that change smoothly with geometry. We can easily achieve this since, at each nuclear geometry, we are free to change the signs of one or more of the three electronic wavefunctions, thus changing the signs of the electronic integrals in Eqs. [1]–[3]. With our phase convention for the two electronic functions $\psi_{\text{elec}}^{(\tilde{a})}$ and $\psi_{\text{elec}}^{(\tilde{b})}$ (which is such that Eq. (26) of Ref. (*8*) is satisfied), we found in Ref. (*3*) that the $\tilde{b} \leftarrow \tilde{a}$ transition moment

$$\bar{\mu}_x^{(\tilde{a}\tilde{b})}\left(\Delta r_{12}^{(\text{ref})}, \Delta r_{32}^{(\text{ref})}, \bar{\rho}\right) = \left\langle \psi_{\text{elec}}^{(\tilde{a})} | \mu_x | \psi_{\text{elec}}^{(\tilde{b})} \right\rangle_{\text{el}} \qquad [4]$$

is negative at all nonlinear nuclear geometries of interest. In the present work, we calculate $\bar{\mu}_x^{(\tilde{a}\tilde{b})}$ along with the transition moments in Eqs. [1]–[3] at each nuclear geometry, and we make the sign changes of the electronic functions so as to make all values of $\bar{\mu}_x^{(\tilde{a}\tilde{b})}$ (at nonlinear geometries) negative. Furthermore, to make the integrals in Eqs. [1]–[3] smooth functions of the vibrational coordinates the signs are chosen so that $\langle \psi_{\text{elec}}^{(\tilde{c})} | \mu_p | \psi_{\text{elec}}^{(\tilde{a})} \rangle_{\text{el}}$ is negative for $r_{32} > r_{12}$ and positive for $r_{32} < r_{12}$, whereas $\langle \psi_{\text{elec}}^{(\tilde{c})} | \mu_q | \psi_{\text{elec}}^{(\tilde{a})} \rangle_{\text{el}}$ and $\langle \psi_{\text{elec}}^{(\tilde{c})} | \mu_x | \psi_{\text{elec}}^{(\tilde{b})} \rangle_{\text{el}}$ are negative for all nonlinear geometries considered.

The two functions $\bar{\mu}_p^{(\tilde{c}\tilde{a})}$ and $\bar{\mu}_q^{(\tilde{c}\tilde{a})}$ vary with the vibrational coordinates in a manner analogous to the p and q components of the dipole moment within one electronic state, and we follow Ref. (*6*) in parameterizing them as

$$\begin{aligned}
&\bar{\mu}_p^{(\tilde{c}\tilde{a})}\left(\Delta r_{12}^{(\text{ref})}, \Delta r_{32}^{(\text{ref})}, \bar{\rho}\right) \\
&\quad = \mu_0^{(p;\tilde{c}\tilde{a})}(\bar{\rho}) + \sum_j \mu_j^{(p;\tilde{c}\tilde{a})}(\bar{\rho}) \Delta r_{j2}^{(\text{ref})} \\
&\qquad + \sum_{j\le k} \mu_{jk}^{(p;\tilde{c}\tilde{a})}(\bar{\rho}) \Delta r_{j2}^{(\text{ref})} \Delta r_{k2}^{(\text{ref})} \\
&\qquad + \sum_{j\le k\le m} \mu_{jkm}^{(p;\tilde{c}\tilde{a})}(\bar{\rho}) \Delta r_{j2}^{(\text{ref})} \Delta r_{k2}^{(\text{ref})} \Delta r_{m2}^{(\text{ref})} \\
&\qquad + \sum_{j\le k\le m\le n} \mu_{jkmn}^{(p;\tilde{c}\tilde{a})}(\bar{\rho}) \Delta r_{j2}^{(\text{ref})} \Delta r_{k2}^{(\text{ref})} \Delta r_{m2}^{(\text{ref})} \Delta r_{n2}^{(\text{ref})} \qquad [5]
\end{aligned}$$

and

$$\begin{aligned}
&\bar{\mu}_q^{(\tilde{c}\tilde{a})}\left(\Delta r_{12}^{(\text{ref})}, \Delta r_{32}^{(\text{ref})}, \bar{\rho}\right) \\
&\quad = \sin\bar{\rho}\Bigg[\mu_0^{(q;\tilde{c}\tilde{a})}(\bar{\rho}) + \sum_j \mu_j^{(q;\tilde{c}\tilde{a})}(\bar{\rho}) \Delta r_{j2}^{(\text{ref})} \\
&\qquad + \sum_{j\le k} \mu_{jk}^{(q;\tilde{c}\tilde{a})}(\bar{\rho}) \Delta r_{j2}^{(\text{ref})} \Delta r_{k2}^{(\text{ref})} \\
&\qquad + \sum_{j\le k\le m} \mu_{jkm}^{(q;\tilde{c}\tilde{a})}(\bar{\rho}) \Delta r_{j2}^{(\text{ref})} \Delta r_{k2}^{(\text{ref})} \Delta r_{m2}^{(\text{ref})} \\
&\qquad + \sum_{j\le k\le m\le n} \mu_{jkmn}^{(q;\tilde{c}\tilde{a})}(\bar{\rho}) \Delta r_{j2}^{(\text{ref})} \Delta r_{k2}^{(\text{ref})} \Delta r_{m2}^{(\text{ref})} \Delta r_{n2}^{(\text{ref})}\Bigg], \qquad [6]
\end{aligned}$$

with $j, k, m, n = 1$ or 3. The angle-dependent coefficients are given by

$$\mu_{jk\ldots}^{(w;\tilde{c}\tilde{a})}(\bar{\rho}) = \sum_{i=0}^{N} w_{jk\ldots}^{(i;\tilde{c}\tilde{a})} (1 - \cos\bar{\rho})^i, \qquad [7]$$

with $w = p$ or q. The function $\mu_0^{(w;\tilde{c}\tilde{a})}(\bar{\rho})$ has $N = 8$, $\mu_j^{(w;\tilde{c}\tilde{a})}(\bar{\rho})$ has $N = 4$, $\mu_{jk}^{(w;\tilde{c}\tilde{a})}(\bar{\rho})$ has $N = 3$, $\mu_{jkm}^{(w;\tilde{c}\tilde{a})}(\bar{\rho})$ has $N = 2$ and $\mu_{jkmn}^{(w;\tilde{c}\tilde{a})}(\bar{\rho})$ has $N = 1$.

The function $\bar{\mu}_x^{(\tilde{c}\tilde{b})}$ behaves analogously to the transition moment $\bar{\mu}_x^{(-+)}$ between the two components of a Renner-degenerate electronic state (see Ref. (*10*)), and we parameterize it as

$$\begin{aligned}
&\bar{\mu}_x^{(\tilde{c}\tilde{b})}\left(\Delta r_{12}^{(\text{ref})}, \Delta r_{32}^{(\text{ref})}, \bar{\rho}\right) \\
&\quad = \sin\bar{\rho}\Bigg[\mu_0^{(x;\tilde{c}\tilde{b})}(\bar{\rho}) + \sum_j \mu_j^{(x;\tilde{c}\tilde{b})}(\bar{\rho}) \Delta r_{j2}^{(\text{ref})} \\
&\qquad + \sum_{j\le k} \mu_{jk}^{(x;\tilde{c}\tilde{b})}(\bar{\rho}) \Delta r_{j2}^{(\text{ref})} \Delta r_{k2}^{(\text{ref})} \\
&\qquad + \sum_{j\le k\le m} \mu_{jkm}^{(x;\tilde{c}\tilde{b})}(\bar{\rho}) \Delta r_{j2}^{(\text{ref})} \Delta r_{k2}^{(\text{ref})} \Delta r_{m2}^{(\text{ref})} \\
&\qquad + \sum_{j\le k\le m\le n} \mu_{jkmn}^{(x;\tilde{c}\tilde{b})}(\bar{\rho}) \Delta r_{j2}^{(\text{ref})} \Delta r_{k2}^{(\text{ref})} \Delta r_{m2}^{(\text{ref})} \Delta r_{n2}^{(\text{ref})}\Bigg], \qquad [8]
\end{aligned}$$

with

$$\mu_{jk\ldots}^{(x;\tilde{c}\tilde{b})}(\bar{\rho}) = \sum_{i=0}^{N} x_{jk\ldots}^{(i;\tilde{c}\tilde{b})} (1 - \cos\bar{\rho})^i, \qquad [9]$$

where the number of summation terms N is given exactly as for Eq. [7].

For CH_2, relations exist between the expansion coefficients in Eqs. [7] and [9], so that the functions $\bar{\mu}_q^{(\tilde{c}\tilde{a})}$ and $\bar{\mu}_x^{(\tilde{c}\tilde{b})}$ are unchanged under the interchange of the two protons, whereas the function $\bar{\mu}_p^{(\tilde{c}\tilde{a})}$ is antisymmetric under this operation.

We obtain values for the $p_{jk\ldots}^{(i;\tilde{c}\tilde{a})}$, $q_{jk\ldots}^{(i;\tilde{c}\tilde{a})}$, and $x_{jk\ldots}^{(i;\tilde{c}\tilde{b})}$ parameters by fitting Eqs. [5]–[9] through the *ab initio* dipole moment values. The results of the fittings (parameter values, standard errors, and the standard deviations of the fittings) are given in Table 1.

III. THE SIMULATION OF THE $\tilde{c} \leftarrow (\tilde{a}/\tilde{b})$ BAND SYSTEM

In order to simulate this band system we combine our program systems MORBID and RENNER. The program system MORBID (Morse Oscillator Rigid Bender Internal Dynamics)

Copyright © 2001 by Academic Press

TABLE 1
Transition Moment Parameters for the $\tilde{c} \leftarrow (\tilde{a}/\tilde{b})$ Band System[a]

$q_0^{(0;\tilde{c}\tilde{a})}$/D	−1.450(13)[b]	$x_0^{(0;\tilde{c}\tilde{b})}$/D	−1.3360(55)
$q_0^{(1;\tilde{c}\tilde{a})}$/D	5.35(28)	$x_0^{(1;\tilde{c}\tilde{b})}$/D	1.700(70)
$q_0^{(2;\tilde{c}\tilde{a})}$/D	−14.1(16)	$x_0^{(2;\tilde{c}\tilde{b})}$/D	−3.46(25)
$q_0^{(3;\tilde{c}\tilde{a})}$/D	20.9(37)	$x_0^{(3;\tilde{c}\tilde{b})}$/D	3.12(31)
$q_0^{(4;\tilde{c}\tilde{a})}$/D	−15.8(36)	$x_0^{(4;\tilde{c}\tilde{b})}$/D	−1.15(13)
$q_0^{(5;\tilde{c}\tilde{a})}$/D	4.6(13)	$x_1^{(0;\tilde{c}\tilde{b})}$/D Å^{-1}	0.4966(92)
$q_1^{(0;\tilde{c}\tilde{a})}$/D Å^{-1}	0.582(11)	$x_{11}^{(0;\tilde{c}\tilde{b})}$/D Å^{-2}	−0.329(51)
$q_1^{(1;\tilde{c}\tilde{a})}$/D Å^{-1}	−0.238(25)	$x_1^{(1;\tilde{c}\tilde{b})}$/D Å^{-1}	0.137(20)
$q_{11}^{(1;\tilde{c}\tilde{a})}$/D Å^{-2}	0.379(53)	$x_{13}^{(0;\tilde{c}\tilde{b})}$/D Å^{-2}	0.754(63)
$q_{13}^{(0;\tilde{c}\tilde{a})}$/D Å^{-2}	1.212(86)	$x_{13}^{(1;\tilde{c}\tilde{b})}$/D Å^{-2}	−1.34(14)
$q_{13}^{(1;\tilde{c}\tilde{a})}$/D Å^{-2}	−2.29(19)	$x_{11}^{(1;\tilde{c}\tilde{b})}$/D Å^{-2}	0.50(11)
St.Dev.[c]/D	0.0037	St.Dev.[c]/D	0.0026
$p_{11}^{(0;\tilde{c}\tilde{a})}$/D Å^{-2}	0.081(16)		
$p_1^{(2;\tilde{c}\tilde{a})}$/D Å^{-1}	−5.394(92)		
$p_1^{(1;\tilde{c}\tilde{a})}$/D Å^{-1}	3.007(47)		
St.Dev.[c]/D	0.0016		

[a] $r_{12}^{(\mathrm{ref})} = r_{32}^{(\mathrm{ref})} = 1.0676$ Å (See Section III).
[b] Quantities in parentheses are standard errors in units of the last digit quoted.
[c] Standard deviation of the fitting.

(*4–7*) was developed to calculate the rotation–vibration energies and transition intensities for an electronic state of a triatomic molecule that remains nondegenerate at linearity. This is appropriate for the $\tilde{c}\ ^1A_1$ state of CH_2. The program system RENNER (*8–10*) was developed to calculate the rovibronic energies and transition intensities for a pair of electronic states of a triatomic molecule that become degenerate at linearity. This is appropriate for the $\tilde{a}\ ^1A_1$ and $\tilde{b}\ ^1B_1$ states of CH_2. Our problem here is to calculate the absorption spectrum for the $\tilde{c} \leftarrow (\tilde{a}/\tilde{b})$ system. This involves using MORBID to calculate the energies and wavefunctions of the $\tilde{c}$ state, and RENNER to calculate the energies and wavefunctions of the $\tilde{a}/\tilde{b}$ pair of Renner interacting states. The line positions are obtained by calculating appropriate energy level differences. The intensities are obtained by calculating the transition moment matrix elements using the calculated wavefunctions and our *ab initio* transition moment surfaces given in Eqs. [5]–[9].

The computer programs MORBID and RENNER are based on theoretical models in which the stretching vibrations are described by a displacement from a *reference configuration* in which the internuclear distances in the CH_2 molecule are fixed at the constant values $r_{12}^{(\mathrm{ref})} = r_{32}^{(\mathrm{ref})}$ (see Section 15.4.7, in particular Fig. 15–14, of Ref. (*20*)). In the MORBID theory, the reference bond lengths are chosen as the equilibrium bond lengths for the isolated electronic state under consideration, whereas in the RENNER theory, the reference bond lengths can be chosen arbitrarily. In order that we obtain the simplest possible expressions for the intensities of the transitions in the $\tilde{c} \leftarrow (\tilde{a}/\tilde{b})$ band system, it is necessary that the reference bond lengths be chosen to be identical for all three electronic states involved. In this way we avoid the effect of axis switching (see, for example, Section 14.1.8 of Ref. (*20*)). Also, the calculations are simplified if we choose the same value of the parameter $a_1 = a_3$ for all three electronic states; this parameter enters into the expression for the potential energy surface (see Eqs. (1)–(7) of Ref. (*4*) and Eqs. (6)–(10) of Ref. (*8*)). Thus, we have refitted the *ab initio* data of Ref. (*11*) to Eqs. (1)–(7) of Ref. (*4*), fixing $a_1 = a_3 = 1.795$ Å^{-1} as used for the $(\tilde{a}/\tilde{b})$ states in Ref. (*3*). In this fitting, the equilibrium internuclear distance of $\tilde{c}\ ^1A_1$ CH_2 was determined to be 1.0676 Å. The potential surfaces for the $(\tilde{a}/\tilde{b})$ states given in Ref. (*3*) were transformed into a form with $r_{12}^{(\mathrm{ref})} = r_{32}^{(\mathrm{ref})} = 1.0676$ Å (keeping $a_1 = a_3 = 1.795$ Å^{-1}). This is an exact transformation carried out by means of Eqs. (13)–(16) of Ref. (*8*). The $\tilde{c}$-state parameters resulting from the refitting of the $\tilde{c}$-state *ab initio* data (which differ slightly from the parameter values given in Ref. (*11*)) and the $(\tilde{a}/\tilde{b})$-state parameters resulting from the transformation (which differ slightly from the parameter values given in Ref. (*3*)) have been used in the simulations reported in the following.

Assuming a Boltzmann distribution with a temperature of 300 K the simulated spectrum of the $\tilde{c} \leftarrow (\tilde{a}/\tilde{b})$ band system is as shown in Fig. 3 for the region 27 500 to 45 000 cm^{-1}. For comparison a simulation of the $\tilde{b} \leftarrow \tilde{a}$ band system for the region 8 000 to 22 000 cm^{-1} is shown in Fig. 4. We have used the potential surfaces, dipole moment, and transition moment surfaces from (*3*), with a temperature of 300 K, for the latter simulation. Note the relative intensities of these two band systems. These band systems involve an electronic transition between an upper state that is linear or quasilinear and a lower state that is well bent. As a result the spectra consist of band progressions $(0, v_2', 0) \leftarrow (0, 0, 0)$ in the upper-state bending quantum number v_2', where we use the linear molecule convention for defining v_2' in Figs. 3 and 4; $v_2^{\mathrm{linear}} = 2v_2^{\mathrm{bent}} + K_a$ for the $\tilde{c}$-state and $v_2^{\mathrm{linear}} =$

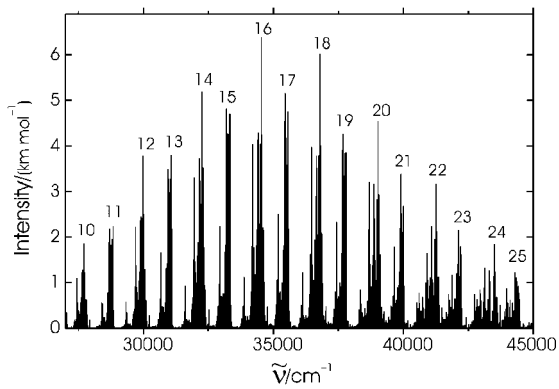

FIG. 3. The simulated $\tilde{c} \leftarrow (\tilde{a}/\tilde{b})$ band system at 300 K without allowing for predissociation or dissociation of any $\tilde{c}$ state levels. The bands form the progression $(0, v_2', 0) \leftarrow (0, 0, 0)$, and the v_2' values are indicated here above each band (v_2' being defined using the linear molecule convention, which for the $\tilde{c}$-state is $v_2^{\mathrm{linear}} = 2v_2^{\mathrm{bent}} + K_a$). In the simulation only transitions having $J \leq 10$ are included.

Copyright © 2001 by Academic Press

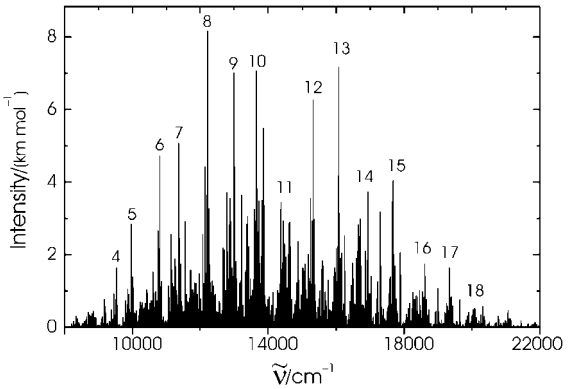

FIG. 4. The simulated $\tilde{b} \leftarrow \tilde{a}$ band system at 300 K. This is calculated using the potential surfaces, dipole moment surfaces, and transition moment surface from (*3*). The bands form the progression $(0, v_2', 0) \leftarrow (0, 0, 0)$, and the v_2' values are indicated here above each band (v_2' being defined using the linear molecule convention which for the $\tilde{b}$-state is $v_2^{\text{linear}} = 2v_2^{\text{bent}} + K_a + 2$). In the simulation only transitions having $J \leq 10$ are included.

$2v_2^{\text{bent}} + K_a + 2$ for the $\tilde{b}$-state (see Eq. [13–177] of (*20*)). For the $\tilde{b} \leftarrow \tilde{a}$ band system Herzberg and Johns (*1*) observed the bands $(0, v_2', 0) \leftarrow (0, 0, 0)$ having $v_2' = 6$, and 8 through 16.

The well-developed band system in Fig. 3 has its maximum intensity at around 35 000 cm^{-1} and at first sight does not seem to be much like the observed spectrum shown in Fig. 1 that occurs around 29 000 cm^{-1}. The bands of this system above about 31 000 cm^{-1} were not simply overlooked in (*1*) since in (*1*) on p. 109 it is stated that "An extensive search was made for other transitions of CH_2 in the region 5000 to 1300 Å." However, the dissociation energy of the $v = N = 0$ level of $\tilde{X}\ ^3B_1$ CH_2 relative to the products $CH(X^2\Pi;\ v = N = 0) + H(^2S)$ was determined by Herzberg (*21*) to have a lower limit of 98 kcal/mol (34 000 cm^{-1}), and *ab initio* calculation (*22*) yields a value very close to this limit. Thus, relative to the $v = J = 0$ level of $\tilde{a}\ ^1A_1$ CH_2, the products $CH(X\ ^2\Pi;\ v = N = 0) + H(^2S)$ are at an energy of about 31 000 cm^{-1}. As shown in Fig. 1 of Beärda *et al.* (*22*) these dissociation products correlate adiabatically with the $\tilde{a}$ and $\tilde{b}$ states of CH_2 but not with the $\tilde{c}$ state. We conclude that the all $\tilde{c}$-state levels above about 31 000 cm^{-1} are broadened by predissociation to the continuum of the $\tilde{a}$ and $\tilde{b}$ states so that transitions to them were not detected in the absorption spectrum obtained in (*1*). Based on the *ab initio* results of (*11*) the observed bands shown in Fig. 1 are assigned as the three $(0, v_2', 0)$–$(0, 0, 0)$ bands of the $\tilde{c} \leftarrow (\tilde{a}/\tilde{b})$ system involving $v_2' = 10$, 11 and 12. The late Alec Douglas observed (*23*) that "predissociation is the last resort of the scoundrel," but we believe that the explanation is sound here bearing in mind the nature and energies of the states involved. This is discussed further in Section IV.

To assign the observed lines rotationally we used a small computer program to search the spectrum for $\tilde{a}$-state combination differences; these differences are given in Table II of Petek *et al.* (*24*). In checking this we noted a misprint in Table II of (*24*): The 3_{21}–3_{03} combination difference should be 54.2063 cm^{-1}. We set a tolerance of 0.15 cm^{-1} for the combination differences; this is based on a comparison between the observed values given in Table 4 of (*1*) and the much more precise ones given in Table II of (*24*). Relating the many $\tilde{a}$-state combination differences found to the line positions and intensities of our simulation we could make the 15 assignments given in Table 2. From the wavenumbers of the assigned lines, which involve seven different $\tilde{c}$-state levels, we calculated $\tilde{c}$-state term values relative to the (0, 0, 0), $J = 0$ level of the $\tilde{a}$-state by making use of the known $\tilde{a}$-state term values from Table II of (*25*). These seven term values T are given in Table 3.

From the term values in Table 3 it is apparent that the rotational spacings in the $v_2^l = 11^{1f}$ level are perturbed. To quantify this we show in Table 4 the values of ν_0, B and D obtained by fitting the observed $J = 1$, 3, and 5 term values of the 11^{1f} level to the usual expansion in $J(J+1) - l^2$. In Table 4 we also show the values of ν_0 and B obtained from fitting the observed $J = 1$ and 3 term values of the 10^0 level, and the constants obtained for the 11^{1f} and 10^0 levels by fitting to the term values obtained using the computer program MORBID with the *ab initio* potential (*11*). It is clear that the observed B value for the 11^{1f} level is anomalous.

We initially thought that we would be able to understand the anomalous B value of the 11^{1f} level as being caused by a

TABLE 2
Assignments of the Observed Spectrum

$\tilde{c}$-state[a] v_2^l, J	$\tilde{a}$-state[b] J_{KaKc}	ν/cm^{-1} obs[c]	Intensity obs[c]	Intensity calc[d]
$10^{2f},2$	2_{12}	27 611.3	2	0.49
$10^{2f},2$	1_{10}	27 639.5	2	1.02
$10^{0},3$	4_{14}	27 683.5	2	0.97
$10^{0},1$	2_{12}	27 719.2	2	1.06
$10^{0},3$	3_{12}	27 721.8	4	1.83
$10^{0},1$	1_{10}	27 747.5	3	1.22
$11^{1f},5$	6_{25}	28 684.4	1	0.35
$11^{1f},5$	5_{23}	28 763.1	3	1.79
$11^{1f},1$	2_{21}	28 765.8	2	1.23
$11^{1e},2$	3_{03}	28 782.1	2	1.34
$11^{1f},3$	3_{21}	28 796.0	3	1.80
$11^{1f},1$	1_{01}	28 846.0	3	1.73
$11^{1f},3$	3_{03}	28 850.3	2	1.56
$11^{1f},5$	5_{05}	28 855.3	1	0.48
$11^{1e},2$	1_{01}	28 868.1	2	1.70

[a] For the $\tilde{c}$-state, $v_1 = v_3 = 0$ and we use linear molecule notation for v_2 [$v_2^{\text{linear}} = 2v_2^{\text{bent}} + K_a$], $\ell = K_a$, and the level is e or f as $J - K_c$ is even or odd, respectively.

[b] For the $\tilde{a}$-state, $v_1 = v_2 = v_3 = 0$.

[c] Ref. (*1*). The observed intensities are not values in km/mol; the numbers given are obtained by estimating the relative darkness of the lines on the photographic plates. See Footnote 1.

[d] Present *ab initio* work in km/mol.

Copyright © 2001 by Academic Press

TABLE 3
$\tilde{c}$-State Term Values T (in cm^{-1})[a]

v_2^l, J	T(obs)
$11^{1f},5$	29 102.7
$11^{1f},3$	28 954.5
$11^{1e},2$	28 886.4
$11^{1f},1$	28 864.3
$10^{0},3$	27 853.9
$10^{0},1$	27 778.8
$10^{2f},2$	27 670.8

[a] Relative to the $v = J = 0$ level of the $\tilde{a}$-state.

perturbation from another vibrational level of the $\tilde{c}$ state, the $(1, 3^{1f}, 2)$ being a nearby candidate. Such a perturbation within the $\tilde{c}$ state is possible, and we find that using the *ab initio* potential the $(0, 15^{1f}, 0)$ level is perturbed by the $(1, 6^{1f}, 2)$ level and has an effective B value of 8.6 cm^{-1}, the $(0, 15^{1e}, 0)$ being unperturbed. However, many attempts at adjusting the parameters in the *ab initio* potential failed at introducing such a large perturbation as is necessary to change the effective B value for the 11^{1f} level from an unperturbed value of about 7.6 cm^{-1} to the observed value of 9.4 cm^{-1}. There is the strong possibility that this perturbation is caused by a vibrational level of the $\tilde{a}/\tilde{b}$ pair of states, and in this region the vibrational energy level density of these states is rather high. We are unable to assign any rotational transitions in the band involving the 12^0 level and presume that it is more strongly perturbed (probably by one or more levels of the $\tilde{a}/\tilde{b}$ pair of states) than the 11^{1f} level. This accords with our supposition that the $(0, 13^1, 0)$ and higher levels of the $\tilde{c}$ state are so strongly nonadiabatically coupled to the $\tilde{a}/\tilde{b}$ continuum as to be predissociated beyond detection in (*1*).

We attempted to assign more of the lines reported in (*1*) by using the fitted effective B and D values to interpolate and extrapolate the levels in the traditional way. However, none of the possible assignments found could be corroborated by an $\tilde{a}$ state

TABLE 4
The Values of ν_0, B, and D (in cm^{-1}) for the 10^0 and 11^{1f} Levels

	observed	*ab initio*[a]
10^0 level		
ν_0	27 764	28 420
B	7.51	7.24
D	–	−0.0014
11^{1f} level		
ν_0	28 846	29 458
B	9.41	7.65
D	0.028	−0.0007

[a] The *ab initio* value of $\nu_0(\tilde{c} - \tilde{a})$ is 17893 cm^{-1} from Ref. (*11*).

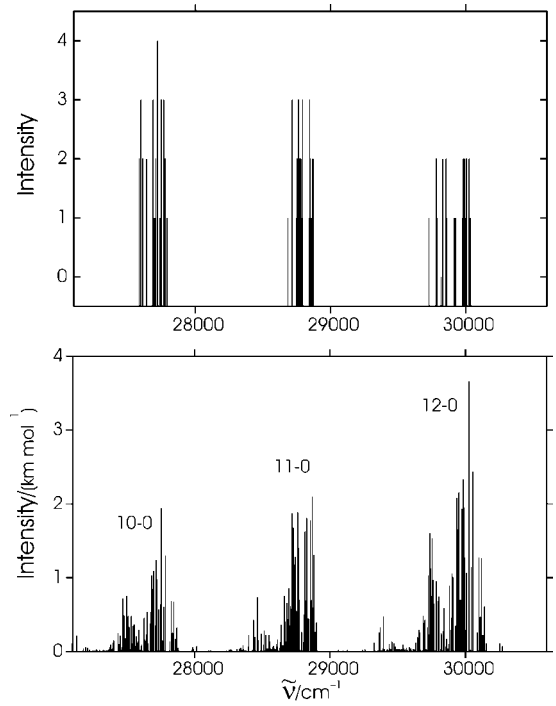

FIG. 5. The comparison of the simulated $\tilde{c} \leftarrow (\tilde{a}/\tilde{b})$ band system using the *ab initio* $\tilde{c}$-state potential with a shift of −618.2 cm^{-1} of the $\tilde{c} \leftarrow \tilde{a}$ band origin ν_0 to 17 274.8 cm^{-1} (lower spectrum) with that observed in (*1*) (upper spectrum; but see Footnote 1). In the simulation only transitions having $J \leq 10$ are included.

combination difference. Extensive attempts at adjusting the $\tilde{c}$ state potential to better fit the observations also failed. There are just too few assigned lines for any meaningful fitting of the $\tilde{c}$ state potential to be achieved.

From the comparison of the observed and *ab initio* results shown in Table 4 it is clear that the *ab initio* $\tilde{c}$–$\tilde{a}$ band origin is about 600 cm^{-1} too high. Adjusting the *ab initio* band origin to 17 274.8 cm^{-1} optimizes the fit of the calculated line positions to those given in Table 2 and with this shift of the band system we show the simulation of the three observed bands in Fig. 5. The results in Table 4 also show that the *ab initio* vibrational interval between the 11^1 and 10^0 levels is about 40 cm^{-1} too small.

IV. DISCUSSION AND SUMMARY

In the Born–Oppenheimer approximation the three lowest singlet states of CH_2 are the $\tilde{a}\ ^1A_1$, $\tilde{b}\ ^1B_1$, and $\tilde{c}\ ^1A_1$ states. The $\tilde{a}$ and $\tilde{b}$ states correlate with a $^1\Delta_g$ state at linearity, and the $\tilde{c}$ state correlates with a $^1\Sigma_g^+$ state. The most precise potential energy surfaces currently available in the spectroscopically accessible regions of nuclear geometries are given in (*3*) for the $\tilde{a}$ and $\tilde{b}$ states, and in (*11*) for the $\tilde{c}$ state. The positions and intensities of the lines in the $\tilde{b} \leftarrow \tilde{a}$ electronic band system have been calculated by using these surfaces together with the *ab initio* dipole moment and transition moment surfaces (*3*); the simulated and observed $\tilde{b} \leftarrow \tilde{a}$ spectra are in good agreement. In the present

Copyright © 2001 by Academic Press

TABLE 5
Important Energies Relative to $C(^1D) + H(^2S) + H(^2S)$

Species	Energy/eV
$C(^1D) + H(^2S) + H(^2S)$	0
$C(^3P) + H(^2S) + H(^2S)$	-1.264^a
$C(^1D) + H_2(X^1\Sigma_g^+; v = J = 0)$	-4.478^b
$CH(X^2\Pi; v = N = 0) + H(^2S)$	$-1.264^a - 3.465^c = -4.729$
$C(^3P) + H_2(X^1\Sigma_g^+; v = J = 0)$	$-1.264^a - 4.478^b = -5.742$
$CH_2[\tilde{a}^1A_1; (0,0,0), J = 0]^d$	$-4.339 - D^f$
$CH_2[\tilde{X}^3B_1; (0,0,0), N = 0]^e$	$-4.729 - D^f$

[a] $E[C(^1D)] - E[C(^3P_0)] = 10\,193.70\ cm^{-1}$ (*26*).
[b] $D_0^0(H_2) = 36\,118.11\ cm^{-1}$ (*27*).
[c] $D_0^0(CH)$ [relative to $C(^3P) + H(^2S)$] = 3.465 eV (*28*).
[d] Energy obtained by adding $T_0(\tilde{a}) = 3147\ cm^{-1}$ (*12*) to the energy[e] of $CH_2(\tilde{X}\,^3B_1; v = N = 0)$.
[e] Energy obtained by subtracting D[f] from the energy of $CH(X\,^2\Pi; v = N = 0) + H(^2S)$.
[f] $D = D_0^0(CH_2)$ for $CH_2[\tilde{X}\,^3B_1; (0, 0, 0), N = 0]$ relative to $[CH(X\,^2\Pi; v = N = 0) + H(^2S)]$. $D \geq 4.25$ eV from (*21*); *ab initio* values are 4.43 eV (*29*) and 4.26 eV (*22*).

paper we calculate *ab initio* the $\tilde{c}$–$\tilde{a}$ and $\tilde{b}$–$\tilde{a}$ electric dipole transition moment surfaces. We then use these in conjunction with calculations of the energy levels and wavefunctions of the states to simulate the $\tilde{c} \leftarrow (\tilde{a}/\tilde{b})$ band system. From this result we can assign the three bands of the near ultraviolet system reported in (*1*) but in order to explain the nonappearance of the higher bands we have to invoke predissociation of the $\tilde{c}$-state levels by nonadiabatic coupling with the dissociation continuum of the $\tilde{a}$ and $\tilde{b}$ states.

In Table 5 we give results from several sources (*12, 21, 22, 26–29*) of relevance to the understanding of the dissociation energies of CH_2. In an *ab initio* study Römelt *et al.* (*29*) determine for $\tilde{X}$-state CH_2 that $D_e[CH + H] = 4.71$ eV and $D_e[C(^3P) + H_2] = 3.56$ eV. Using the zero point energies of CH, H_2, and CH_2 in their ground electronic states gives D_0^0 values of 4.43 and 3.37 eV, respectively, and places the products $CH(X^2\Pi; v = N = 0) + H(^2S)$ at an energy of 4.04 eV (32 600 cm^{-1}) above the $[(0, 0, 0), J = 0]$ level of $\tilde{a}$-state CH_2. In another *ab initio* calculation Beärda *et al.* (*22*) obtain $D_e[CH + H] = 4.54$ eV, which gives $D_0^0 = 4.26$ eV; this is in close agreement with the experimental upper limit (*21*) of 4.25 eV.

From Table 5 we see that the products $C(^1D) + H_2(X^1\Sigma_g^+; v = J = 0)$ are at an energy of 0.251 eV (2020 cm^{-1}) above the products $CH(X\,^2\Pi; v = N = 0) + H(^2S)$; we also see that this energy separation would be more accurately known if the dissociation energy of CH were more accurately determined. As shown in Fig. 1 of Beärda *et al.* (*22*) the $\tilde{a}$ and $\tilde{b}$ states of CH_2 adiabatically dissociate to both of these products, but the $\tilde{c}$ state cannot adiabatically dissociate to the products at the lower energy. Taking $D_0^0 = 4.26$ eV from (*22*) means that the products $CH(X\,^2\Pi; v = N = 0) + H(^2S)$ are at an energy of 3.87 eV (31 200 cm^{-1}) above the $[(0, 0, 0), J = 0]$ level of $\tilde{a}$-state CH_2. This agrees with the energy in the $\tilde{c} \leftarrow \tilde{a}$ band system above which the bands disappear in the spectrum of (*1*). Thus we suggest that all $\tilde{c}$ state levels above the adiabatic dissociation energy limit for the $\tilde{a}$ and $\tilde{b}$ states are broadened beyond detection in (*1*) as a result of nonadiabatic dissociation (predissociation) of $\tilde{c}$-state CH_2 into the $\tilde{a}/\tilde{b}$ continuum formed by $CH(X\,^2\Pi; v = N = 0) + H(^2S)$.

The adiabatic dissociation path of the $\tilde{a}$ state has not been studied, but that for the analogous $\tilde{X}\,^1A_1$ state of SiH_2 is barrierless (*30*). As well as the lack of a barrier in the $\tilde{a}$-state adiabatic dissociation path, it is also important to investigate the variation in energy separation, and even (possibly) of the energy ordering, of the low-lying singlet states of CH_2 as a function of nuclear geometry. As well as considering a possible seam of crossing between the $\tilde{c}$ state and another singlet state of different symmetry, it is also necessary to consider the minimum points of avoided crossing between the $\tilde{a}$ and $\tilde{c}$ states. The rapid changes in the electronic wavefunctions of the $\tilde{a}$ and $\tilde{c}$ states in the region of such an avoided crossing would lead to large nonadiabatic coupling. The dissociation dynamics of the triplet states of CH_2 have been studied *ab initio* by Beärda *et al.* (*22*), and there is a later theoretical study of the ground state of CH_2 by Harding *et al.* (*31*). For the low-lying singlet and triplet states of SiH_2 there is an experimental and theoretical study of the dissociation dynamics by Francisco *et al.* (*30*), but there is no similar study for singlet CH_2.

The vibrational assignment of the three near ultraviolet bands of CH_2, based on our simulation of the band system using the *ab initio* $\tilde{c}$-state potential surface (*11*), is that they form part of the bending vibrational progression $(0, v_2, 0) \leftarrow (0, 0, 0)$ having $v_2 = 10$, 11, and 12. Following the identification of $\tilde{a}$-state combination differences, and from the appearance of our simulated spectrum, we can make some rotational assignments; these are given in Table 2. The $\tilde{c}$-state potential surface leads to a simulated spectrum that is compared to the observations in Fig. 5. The vibrational assignment requires that we shift $\nu_0(\tilde{c}$–$\tilde{a})$ by about $-600\ cm^{-1}$ from the *ab initio* value (*11*) of 17 893 cm^{-1}. The v_2' vibrational assignments could be changed up or down by two[2] but then we would have to shift ν_0 by about $-2900\ cm^{-1}$ or $+1600\ cm^{-1}$, respectively, from the *ab initio* value, and this is not reasonable given the level of the *ab initio* calculation in (*11*).

There is not very satisfactory agreement between our simulated spectrum and the observed one. Although in judging the comparison shown in Fig. 5 we have to bear in mind the approximate nature of the plotted "observed" intensities (see Footnote 1). The levels of the $\tilde{c}$ state are embedded in the levels of the $\tilde{a}$ and $\tilde{b}$ singlet states as well in the continuum of the $\tilde{X}$ triplet state. Random perturbations by the levels of the $\tilde{a}$ and $\tilde{b}$ states are quite possible. The triplet state dissociation limit $[C(^3P) + H_2]$ occurs at an energy of about 23 000 cm^{-1} above the $[(0, 0, 0), J = 0]$ level of the $\tilde{a}$ state, so that $\tilde{c}$-state

[2] The v_2' numbering cannot be changed by one since our rotational assignments imply that v_2' is even for the band observed at lowest wavenumber.

Copyright © 2001 by Academic Press

predissociation by singlet–triplet interaction would cause a broadening and weakening of the lines in the observed near-ultraviolet bands. It is clear that the $\tilde{c}$ state is significantly perturbed since the B value of the 11^{1f} state is anomalous, and since we cannot assign the structure in the band involving the 12^0 level. We cannot hope to simulate the observed spectrum satisfactorily without taking the perturbations into account.

In conclusion, we can assign the near-ultraviolet band system of CH_2 observed by Herzberg and Johns (*1*) as the $\tilde{c} \leftarrow (\tilde{a}/\tilde{b})$ band system, which they suggest. We can vibrationally assign the bands and make some rotational assignments. Our simulation of the band system leads us to conclude that levels of the $\tilde{c}$ state above the adiabatic dissociation limit of the $\tilde{a}$ and $\tilde{b}$ states (to CH + H) are predissociated to such an extent that their observation in absorption was not possible in (*1*) and that the observed bound levels $(0, 11^{1f}, 0)$ and $(0, 12^0, 0)$ of the $\tilde{c}$ state are perturbed, most probably by levels of the $\tilde{a}$ and $\tilde{b}$ states.

Further experimental studies of the spectra and dissociation dynamics of singlet CH_2 are warranted, as are further theoretical studies of the singlet state potential energy surfaces away from the equilibrium nuclear configurations. We are undertaking the latter. If it is possible to chemically generate CH_2 radicals with significant $\tilde{c}$ state population then attempts could be made to observe the $\tilde{c} \rightarrow \tilde{a}/\tilde{b}$ emission band system. This would give information on the lowest levels of the $\tilde{c}$ state and on the levels of the $\tilde{a}/\tilde{b}$ states near the top of the barrier to linearity. We simulate this emission spectrum in Fig. 6 where we have presumed an initial 300 K Boltzmann population distribution in the $\tilde{c}$ state. Another way of interrogating the $\tilde{c}$ state would be a double resonance study in which known near infrared $\tilde{b} \leftarrow \tilde{a}$ absorption lines (see Table 1 of (*2*)) are pumped and a second laser used to probe $\tilde{c} \leftarrow \tilde{b}$ absorption from each of the pumped $\tilde{b}$ state levels. We can provide predicted line positions which would be of help in the search for such a spectrum.

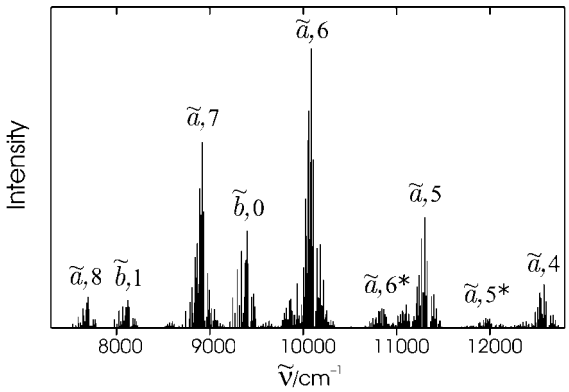

FIG. 6. A simulation of the $\tilde{c} \rightarrow (\tilde{a}/\tilde{b})$ emission band system using the *ab initio* (*11*) $\tilde{c}$-state potential. An initial 300-K Boltzmann population distribution in the $\tilde{c}$ state is assumed; this means that there is only significant population in the $(v_1, v_2^{\text{bent}}, v_3) = (0, 0, 0)$ level. The notation gives the value of v_2^{bent} for the $\tilde{a}$ state and for the $\tilde{b}$ state. For the two bands marked by an asterisk the upper ($\tilde{c}$) state value of $K_a = l$ is one, whereas for the other bands it is zero. In this simulation only transitions having $J \leq 10$ are included.

ACKNOWLEDGMENTS

We are grateful for very helpful correspondence from Wesley Allen and Trevor Sears. This work was supported in part by the Deutsche Forschungsgemeinschaft, the Fonds der Chemischen Industrie, and the U.S. National Science Foundation. P.J. is grateful to the Steacie Institute for Molecular Sciences for hospitality.

REFERENCES

1. G. Herzberg and J. W. C. Johns, *Proc. Roy. Soc. London, Ser. A.* **295,** 107–128 (1966).
2. K. Kobayashi, L. D. Pride, and T. J. Sears, *J. Phys. Chem. A.* **104,** 10 119–10 124 (2000).
3. J.-P. Gu, R. J. Buenker, M. Brumm, G. Osmann, P. R. Bunker, and P. Jensen, *J. Mol. Struct.* **517–518,** 247–264 (2000).
4. P. Jensen, *J. Mol. Spectrosc.* **128,** 478–501 (1988).
5. P. Jensen, *J. Chem. Soc. Faraday Trans. 2* **84,** 1315–1340 (1988).
6. P. Jensen, *J. Mol. Spectrosc.* **132,** 429–457 (1988).
7. P. Jensen, *in* "Methods in Computational Molecular Physics" (S. Wilson and G. H. F. Diercksen, Eds.). Plenum, New York, 1992.
8. P. Jensen, M. Brumm, W. P. Kraemer, and P. R. Bunker, *J. Mol. Spectrosc.* **171,** 31–57 (1995).
9. M. Kolbuszewski, P. R. Bunker, P. Jensen, and W. P. Kraemer, *Mol. Phys.* **88,** 105–124 (1996).
10. G. Osmann, P. R. Bunker, P. Jensen, and W. P. Kraemer, *Chem. Phys.* **225,** 33–54 (1997).
11. P. R. Bunker, P. Jensen, Y. Yamaguchi, and H. F. Schaefer III, *J. Phys. Chem.* **100,** 18 088–18 092 (1996).
12. P. Jensen and P. R. Bunker, *J. Chem. Phys.* **89,** 1327–1332 (1988).
13. R. J. Buenker and S. D. Peyerimhoff, *Theor. Chim. Acta* **35,** 33–58 (1974).
14. R. J. Buenker and S. D. Peyerimhoff, *Theor. Chim. Acta* **39,** 217–228 (1975).
15. S. Krebs and R. J. Buenker, *J. Chem. Phys.* **103,** 5613–5629 (1995).
16. R. J. Buenker, *in* "Proceedings of the Workshop on Quantum Chemistry and Molecular Physics, Wollongong, Australia" (P. Burton, Ed.). University Press, Wollongong, 1980.
17. R. J. Buenker, *in* "Current Aspects of Quantum Chemistry" (R. Carbó Ed.), Studies in Physical and Theoretical Chemistry, Vol. 21, p. 17. Elsevier, Amsterdam, 1981.
18. R. J. Buenker and R. A. Phillips, *THEOCHEM* **123,** 291–300 (1985).
19. T. H. Dunning, Jr., *J. Chem. Phys.* **90,** 1007–1023 (1989).
20. P. R. Bunker and P. Jensen, "Molecular Symmetry and Spectroscopy." NRC Research Press, Ottawa, 1998.
21. G. Herzberg, *Can. J. Phys.* **39,** 1511–1513 (1961).
22. R. A. Beärda, M. C. van Hemert, and E. F. van Dishoeck, *J. Chem. Phys.* **97,** 8240–8249 (1992).
23. A. E. Douglas, personal communication.
24. H. Petek, D. J. Nesbitt, C. B. Moore, F. W. Birss, and D. A. Ramsay, *J. Chem. Phys.* **86,** 1189–1205 (1987).
25. H. Petek, D. J. Nesbitt, D. C. Darwin, and C. B. Moore, *J. Chem. Phys.* **86,** 1172–1188 (1987).
26. C. E. Moore, "Atomic Energy Levels" Vol. 1. National Bureau of Standards, Washington. DC., 1949.
27. A. Balakrishnan, V. Smith, and B. P. Stoicheff, *Phys. Rev. Lett.* **68,** 2149–2152 (1992).
28. K. P. Huber and G. Herzberg, "Constants of Diatomic Molecules." Van Nostrand Reinhold, New York, 1979.
29. J. Römelt, S. D. Peyerimhoff, and R. J. Buenker, *Chem. Phys.* **54,** 147–158 (1981).
30. J. S. Francisco, R. Barnes and J. W. Thoman, Jr., *J. Chem. Phys.* **88,** 2334–2341 (1988).
31. L. B. Harding, R. Guardagnini, and G. C. Schatz, *J. Phys. Chem.* **97,** 5472–5481 (1993).

Copyright © 2001 by Academic Press